



Contents lists available at ScienceDirect

Chinese Chemical Letters

journal homepage: www.elsevier.com/locate/cclet

Original article

Nanosized Pd assembled on superparamagnetic core–shell microspheres: Synthesis, characterization and recyclable catalytic properties for the Heck reaction

Qi Hao Yang, Da Shi, Sheng-Fu Ji*, Dan-Ni Zhang, Xue-Fei Liu

State Key Laboratory of Chemical Resource Engineering, Beijing University of Chemical Technology, Beijing 100029, China

ARTICLE INFO

Article history:

Received 31 January 2014

Received in revised form 18 April 2014

Accepted 29 April 2014

Available online xxx

Keywords:

Nano-Pd

Superparamagnetic

Core–shell

Catalyst

Heck reaction

ABSTRACT

A series of magnetically recyclable Pd/Fe₃O₄@γ-Al₂O₃ catalysts were synthesized using the superparamagnetic Fe₃O₄@γ-Al₂O₃ core–shell microspheres as the supporter and nano-Pd particles assembled on γ-Al₂O₃ shell as the active catalytic component. The structure of the catalysts was characterized by X-ray diffraction (XRD), transmission electron microscopy (TEM), N₂ adsorption–desorption and vibrating sample magnetometer (VSM). The catalytic activity and the recyclability properties of the catalysts for the Heck coupling reaction with aryl bromides and the olefins were investigated. The results show that the microspheres of the magnetic Pd/Fe₃O₄@γ-Al₂O₃ catalysts were about 400 nm and the nano-Pd particles assembled on γ-Al₂O₃ shell were about 3–4 nm in size. The saturation magnetization (MS) of the magnetic catalysts was sufficiently high to allow magnetic separations. In the Heck coupling reactions, the magnetic Pd/Fe₃O₄@γ-Al₂O₃ catalysts exhibited good catalytic activity and recyclability. With Pd/Fe₃O₄@γ-Al₂O₃ (0.021 mol%) catalyst, the bromobenzene conversion and product yield reached about 96.8% and 91.2%, respectively, at 120 °C and in 14 h. After being recycled for six times, the conversion of bromobenzene and the recovery of the catalyst were about 80% and 90%, respectively. The nano-Pd particles were kept well dispersed in the used Pd/Fe₃O₄@γ-Al₂O₃ catalysts.

© 2014 Sheng-Fu Ji. Published by Elsevier B.V. on behalf of Chinese Chemical Society. All rights reserved.

1. Introduction

The Heck reaction catalyzed by the noble metal Pd is one of the most important coupling reactions in organic syntheses [1,2]. Homogeneous and heterogeneous Pd catalysts are often used in the Heck reaction. However, homogeneous catalysts are used in less than one fifth of industrial applications due to the facts that the homogeneous catalysts are easily lost after reaction, difficult to separate from the reaction system and certainly costly [3]. Generally, Pd catalysts are initially synthesized as heterogeneous catalysts followed by loading onto active carbon [4], metal oxides [5], zeolites [6], polymers [7], or clay [8].

Magnetic catalysts have the incomparable advantages over the traditional catalysts because of their high activity, magnetic recyclability, and reusability. Research on the magnetic nanocatalysts for the Heck reaction had been reported earlier [9,10].

However, due to their high specific surface areas and magnetic properties, magnetic nanoparticles are often easily self-agglomerated [11]. Therefore, SiO₂, C, and metal oxides, polymers are usually used to modify the magnetic nanoparticles and to obtain magnetic nanoparticles with special surface properties that still keep their dispersiveness [12–15]. γ-Al₂O₃ has been used as supporter, adsorbent, and catalyst, owing to its low cost, good chemical stability, high surface area, acidic sites, and controllable synthetic process [16–19]. In the catalytic industry, γ-Al₂O₃ is an ideal supporter. Particularly, the catalysts that are formed by loading the noble metal on the γ-Al₂O₃ were used in organic reactions [19–22]. It is still difficult, however, to separate the catalyst from the liquid phase after the reaction. In our previous research, we found an easy way to synthesize monodispersed Fe₃O₄ [23], which had uniformed diameter. Thus we hypothesized that if we could coat the Fe₃O₄ with γ-Al₂O₃ to obtain core–shell structures, and then load Pd onto the Fe₃O₄@γ-Al₂O₃ nanospheres, the resulting catalysts would combine their advantages of high activity, excellent mesoporous structure, magnetic recyclability, and reusability.

* Corresponding author.

E-mail address: jjsf@mail.buct.edu.cn (S.-F. Ji).

In this paper, we illustrated the construction of magnetically recyclable Pd/Fe₃O₄@γ-Al₂O₃ nanocomposites possessed the core-shell structure. To evaluate the activity and the stability of the Pd/Fe₃O₄@γ-Al₂O₃ nanocomposites, the Heck coupling reactions were chosen as the model reaction. Results showed that the catalyst could be easily separated from the reaction system by employing an external magnetic field, because of the superparamagnetic behavior of Fe₃O₄. Furthermore, it can be reused for several cycles with sustained selectivity and activity.

2. Experimental

2.1. Synthesis of Fe₃O₄@γ-Al₂O₃

Fe₃O₄ was synthesized according to a slightly modified solvothermal method [23]. Briefly: FeCl₃·6H₂O (10.8 g), NaAc (28.8 g) and cetyltrimethyl ammonium bromide (CTAB, 0.014 g) were dissolved in 400 mL of glycol under stirring. The obtained homogeneous yellow solution was transferred into a Teflon-lined stainless-steel autoclave. The autoclave was sealed and heated at 200 °C under 400 rpm stirring speed. After heating for 12 h, the autoclave was cooled naturally to room temperature. The obtained black magnetic particles were separated with a permanent magnet, washed with ethanol six times, and dried in vacuum at 60 °C for 24 h.

The obtained Fe₃O₄ particles (0.1 g) were dispersed in an aluminum isopropoxide (AIP) ethanol solution (60 mL, 0.016 mol/L) under ultrasonication. After 30 min, the solution was transferred to a three-neck flask (250 mL) and stirred for 12 h at 45 °C to obtain the Fe₃O₄ particles whose surface was saturated with AIP. Subsequently, 50 mL of ethanol/water (5/1, V/V) was added into the solution, and the mixture was allowed to stir for another 1 h to complete the hydrolysis of AIP. Then the mixture was transferred to a Teflon-sealed autoclave and heated at 80 °C for 20 h. The obtained particles were separated with a permanent magnet, washed several times with deionized water and ethanol, and then dried in vacuum at 50 °C for 12 h. After that the products were put into a tube furnace and the system was purged with N₂. Then the tube furnace was heated from room temperature to 500 °C (1 °C/min) under the N₂ (5 mL/min) ambience, and kept at 500 °C for 4 h. After cooling to room temperature naturally, the Fe₃O₄@γ-Al₂O₃ was collected.

2.2. Preparation of Pd/Fe₃O₄@γ-Al₂O₃

0.1 g of the obtained Fe₃O₄@γ-Al₂O₃ particles was dispersed in a 2.5 mL PdCl₂ aqueous solution (0.6 mg/mL) under ultrasonication. After 30 min, the solution was diluted to 100 mL and transferred to a three-neck flask, stirred for 12 h under 25 °C, separated by a permanent magnet, and finally dried in vacuum at 100 °C for 12 h. The obtained products were put into a tube furnace, which was purged with H₂. Then the tube furnace was heated from room temperature to 200 °C (1 °C/min) under the H₂ (5 mL/min) ambience, and kept at 200 °C for 3 h. After cooling to room temperature, Pd/Fe₃O₄@γ-Al₂O₃ (1.5 wt%) was collected. By changing the volume of PdCl₂ added, we synthesized a series of Pd/Fe₃O₄@γ-Al₂O₃ catalysts with different Pd loadings in 1.5%, 3.0%, 4.5%, 6.0%, respectively. They were marked as Pd-1, Pd-2, Pd-3, Pd-4, respectively.

2.3. Catalytic reaction

For the Heck reactions, 10 mg of Pd/Fe₃O₄@γ-Al₂O₃ catalyst, arylhalide, olefin, dodecane (as an internal standard substance), and base were added to the solvent. The reaction was carried out under reflux condition. The effects of Pd content, solvents,

substrates, and time were investigated individually. The catalyst was collected by an external permanent magnet, and the product was analyzed by gas chromatography (GC). For recycling, the collected catalyst was washed with tetrahydrofuran and separated by an external permanent magnet, then dried under vacuum at 60 °C for 12 h. Then the catalysts were utilized for another run of catalytic testing. Each time, catalyst loss was measured by precision electronic balance.

2.4. Characterizations

The X-ray diffraction (XRD) pattern was collected on a D/Max 2500 VB 2+/PC diffractometer (Rigaku, Japan) with Cu-Kα irradiation (λ = 1.5418 Å, 200 kV, 50 mA) with 2θ values between 10° and 80°. Transmission electron microscopy (TEM) was performed with a JEOL (JEM-2100) transmission electron microscope (JEOL, Japan) operated at 200 kV accelerating voltage. The N₂ adsorption-desorption analysis was conducted with an ASAP 2020 M automatic specific surface area and aperture analyzer (MICROMERITICS, USA). Magnetic properties of the samples were measured using a vibrating sample magnetometer (VSM; Lake Shore Model 7400, USA) under magnetic fields up to 18 kOe. The Pd loading amount was determined by inductively coupled plasma mass spectrometry (ICP-MS, SPECTRO ARCOS EOP; SPECTRO Analytical Instruments GmbH, Germany).

3. Results and discussion

3.1. The structure of the catalyst

Fig. 1 shows the crystallinity and phase composition of the samples by X-ray powder diffraction (XRD). The peaks of all samples could be indexed to face center cubic magnetite phase (Fe₃O₄; JCPDS No. 19-0629). The extra weak diffraction peaks at 45.9°, 66.7° could be indexed to the characteristic diffraction peaks of γ-Al₂O₃ (2θ = 37.6°, 45.7°, 66.6°; PDF No. 10-425), which indicates that both Fe₃O₄ and γ-Al₂O₃ had been obtained [24]. Since the peak at 2θ = 37.6° was so close to the Fe₃O₄ characteristic diffraction peak that they could not be distinguished by the XRD. Fig. 1 shows that the Pd/Fe₃O₄@γ-Al₂O₃ nanocomposites displayed the characteristic diffraction peaks indexed to the Pd (0), which suggested the presence of Pd (0) on Pd/Fe₃O₄@γ-Al₂O₃ composites. The intensity became stronger as the concentration of Pd increased.

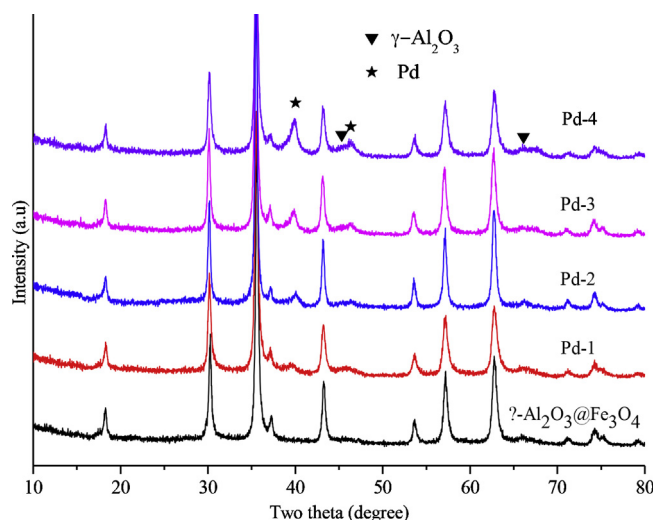


Fig. 1. Wide-angle XRD patterns of Pd/Fe₃O₄@γ-Al₂O₃ with different Pd loading.

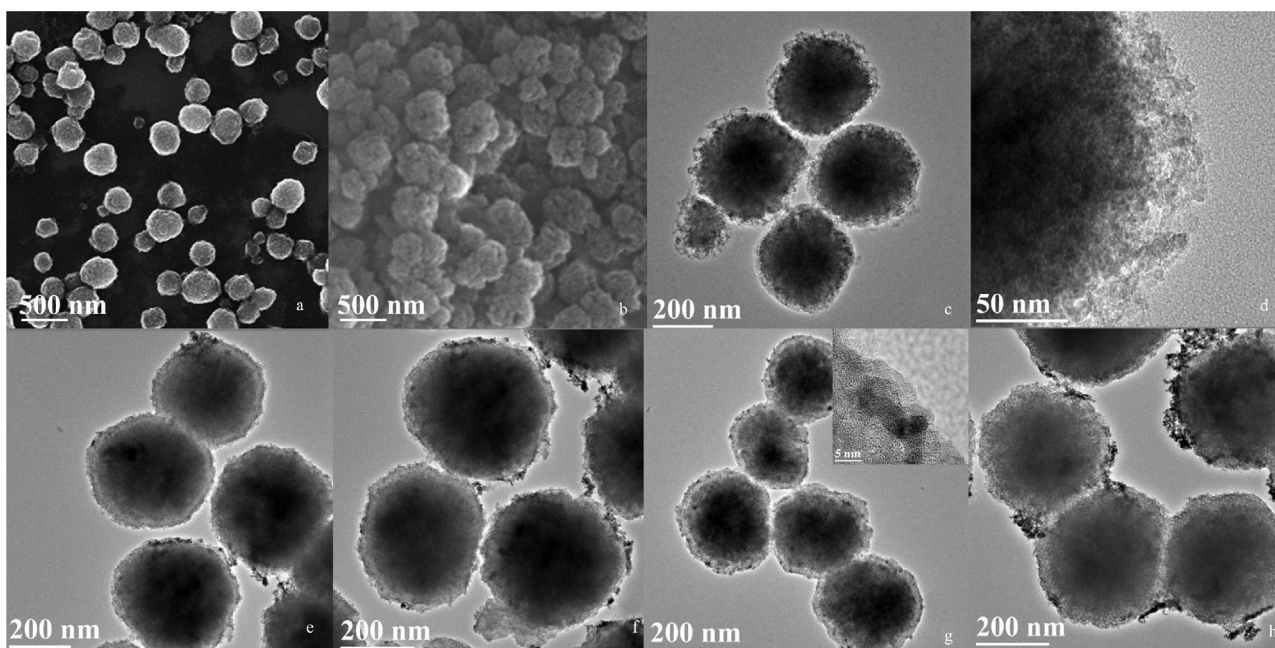


Fig. 2. SEM images of Fe_3O_4 (a) and $\text{Fe}_3\text{O}_4@ \gamma\text{-Al}_2\text{O}_3$ (b); TEM images of $\text{Fe}_3\text{O}_4@ \gamma\text{-Al}_2\text{O}_3$ (c, d); TEM images of Pd-1 (e), Pd-2 (f), Pd-3 (g), Pd-4 (h).

Fig. 2 shows typical SEM and TEM images of $\text{Fe}_3\text{O}_4@ \gamma\text{-Al}_2\text{O}_3$ and Pd/ $\text{Fe}_3\text{O}_4@ \gamma\text{-Al}_2\text{O}_3$. It was easily observed, as in Fig. 2a-d, that the diameters of the as-synthesized Fe_3O_4 nanoparticles were about 300 nm with a narrow size distribution, and that the thickness of the $\gamma\text{-Al}_2\text{O}_3$ shell was about 40 nm. If observed carefully we could find some porous structures, which resulted from the stacking of smaller $\gamma\text{-Al}_2\text{O}_3$ particles on the outer space of the $\gamma\text{-Al}_2\text{O}_3$ shell. Fig. 2e-f illustrated the TEM images of different loading of Pd/ $\text{Fe}_3\text{O}_4@ \gamma\text{-Al}_2\text{O}_3$ (Pd-1, Pd-2, Pd-3, Pd-4). One could see from the figure that there were some small Pd clusters, which stacked by smaller Pd nano-particles with the average diameter of 3-4 nm on the surface of $\text{Fe}_3\text{O}_4@ \gamma\text{-Al}_2\text{O}_3$. As the Pd loading increases, the clusters tend to increase. However, excess Pd loading may lead to Pd cluster agglomerating.

Nitrogen adsorption-desorption isotherms of all the samples are illustrated in Fig. 3, and the textural and structural

characteristics of Pd/ $\text{Fe}_3\text{O}_4@ \gamma\text{-Al}_2\text{O}_3$ with different Pd loading were shown in Table 1. The isotherms of all the samples are type III (definition by IUPAC). The appearance of type 3-H hysteresis loops in isotherms was indicated because there was no presence of orderly mesoporous structures in $\text{Fe}_3\text{O}_4@ \gamma\text{-Al}_2\text{O}_3$ magnetic particles. After Pd was loaded, the BET surface area decreased compared with $\text{Fe}_3\text{O}_4@ \gamma\text{-Al}_2\text{O}_3$ magnetic particles. As the Pd loading increased, the decrease of BET surface area became more significant. However, the pore volume remained constant, indicating that the Pd clusters were loaded on the surface of the $\text{Fe}_3\text{O}_4@ \gamma\text{-Al}_2\text{O}_3$ [25], which was consistent with the TEM results.

Magnetic properties of the samples were investigated by a vibrating sample magnetometer (VSM) at room temperature with the applied magnetic field ranging from -18,000 to 18,000 Oe. As illustrated in Fig. 4, all samples were superparamagnetic nanoparticles. Compared with Fe_3O_4 , the saturation magnetization (M_S) intensity of the $\gamma\text{-Al}_2\text{O}_3@ \text{Fe}_3\text{O}_4$ and Pd-1, Pd-2, Pd-3, Pd-4 successively decreased. Even so, the M_S of the Pd/ $\gamma\text{-Al}_2\text{O}_3@ \text{Fe}_3\text{O}_4$ was adequately high to allow its easy separation from the reaction system.

3.2. Catalytic performance of Pd/ $\text{Fe}_3\text{O}_4@ \gamma\text{-Al}_2\text{O}_3$

The Heck reaction of bromobenzene with styrene was carried out as a model reaction to evaluate the catalytic ability of the

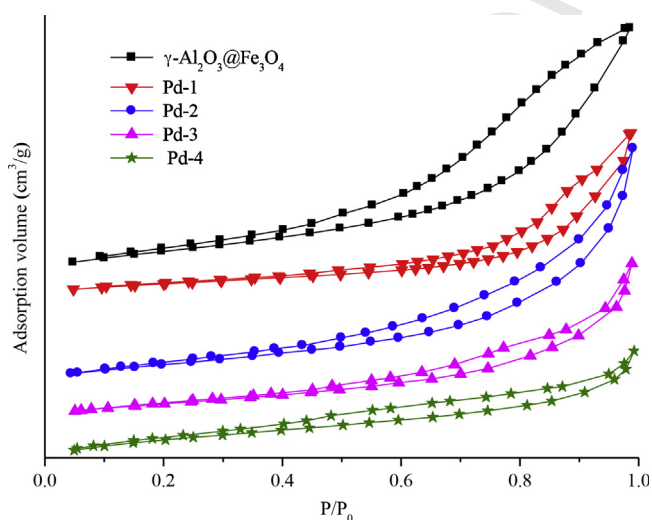


Fig. 3. N_2 adsorption-desorption isotherms of Pd/ $\text{Fe}_3\text{O}_4@ \gamma\text{-Al}_2\text{O}_3$ with different Pd loading.

Table 1
Textural and structural characteristics of Pd/ $\text{Fe}_3\text{O}_4@ \gamma\text{-Al}_2\text{O}_3$ with different Pd loading.

Catalyst	Palladium (wt%)	Textural and structural characteristics		
		S_{BET} (m^2/g)	V_{BJH} (cm^3/g)	D_v (nm)
Fe_3O_4	-	468.6	0.35	2.3
$\text{Fe}_3\text{O}_4@ \gamma\text{-Al}_2\text{O}_3$	-	179.3	0.26	5.9
Pd-1	1.5	166.8	0.24	5.7
Pd-2	3.0	153.9	0.23	5.8
Pd-3	4.5	138.6	0.23	5.8
Pd-4	6.0	124.5	0.25	5.7

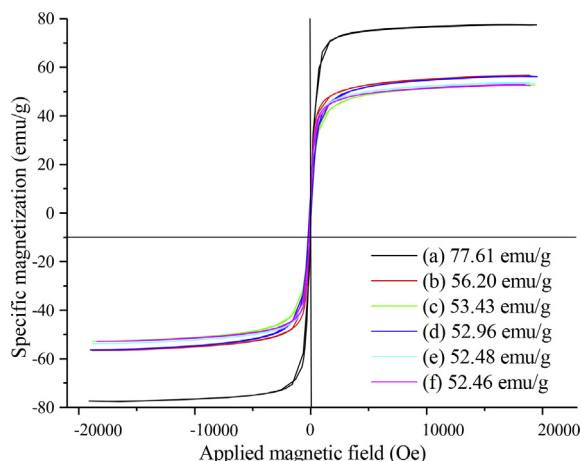


Fig. 4. Magnetization curves of Pd/Fe₃O₄@γ-Al₂O₃ with different Pd loading. (a) Fe₃O₄, (b) Fe₃O₄@γ-Al₂O₃, (c) Pd-1, (d) Pd-2, (e) Pd-3, (f) Pd-4.

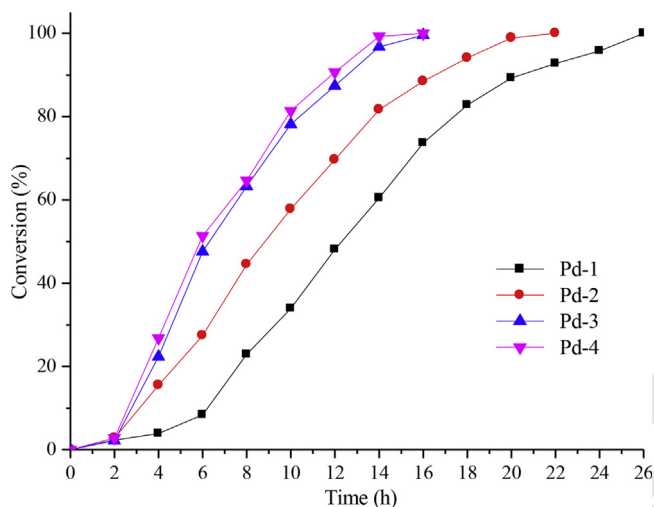


Fig. 5. Time-dependent Heck activities of Pd/Fe₃O₄@γ-Al₂O₃ catalysts with different Pd loading.

Pd/Fe₃O₄@γ-Al₂O₃. We systematically investigated the effects of Pd content, temperature, base, and solvent on the reaction. Time-dependent Heck reaction activity of the Pd/Fe₃O₄@γ-Al₂O₃ catalysts with different Pd loadings is shown in Fig. 5, with reaction conditions: 10 mg of Pd/Fe₃O₄@γ-Al₂O₃ catalyst, bromobenzene (20 mmol), styrene (30 mmol), dodecane (10 mmol, as internal standard substance), Na₂CO₃ (24 mmol), NMP (*N*-methyl-2-pyrrolidone, 40 mL), and reaction temperature (120 °C). It can be observed from Fig. 5 that the conversion of bromobenzene increased to as much as 100% given sufficient reaction time. The difference is that with the increase of Pd content, the conversion

rate of bromobenzene became faster. The conversion of bromobenzene increased slowly with a low Pd/bromobenzene molar ratio (Fig. 5a, 0.007%) and needed 24 h to finish the reaction, whereas a higher Pd/bromobenzene molar ratio (Fig. 5c, 0.021%) needed 14 h to finish the reaction. Furthermore, an increase in the Pd/bromobenzene molar ratio could not help to decrease the reaction time (Fig. 5d). For the Pd atom utilization, the conversion of Pd-1–Pd-4 was 60.5%, 81.7%, 96.8%, 99.3% in 14 h, respectively. The conversion of bromobenzene rose to about 18% when the Pd content increased 1.5 wt%, and it decreased with the increased Pd content, which means that the dominant factor was changed from the number of active sites to the mass transfer rate of the substrates [26]. In addition, increasing the Pd content led to serious Pd clusters agglomerating (Pd-4) judged by the TEM image, which suggests that the a Pd content of Pd-3 (4.5 wt%) was adequate to catalyze the reaction.

Table 2 show the Heck activity of bromobenzene and styrene catalyzed by Pd-3 catalysts under different reaction conditions. As we can see from entry 1 to entry 4, temperature was a key factor for the Heck reaction. As the temperature rose, the conversion of bromobenzene increased; when the temperature reached to 120 °C, a 96.8% conversion of bromobenzene was achieved with a high yield of 91.2%. High temperature enabled more molecule activated, thus increasing the reaction rate. For the purposes of energy saving and prolonging the life of the catalyst, lower reaction temperatures are more desirable, thus 120 °C was the best reaction temperature for the Pd-3 catalyst. It was also found that inorganic base was more effective than organic base, and Na₂CO₃ was the ideal base among Na₂CO₃, NaOAc, and Et₃N tested (entry 4 to entry 6)

Table 3 shows a comparison of the activity and reaction conditions of supported Pd catalysts in the Heck reaction of bromobenzene with styrene that had been published in the literature. As we can see from the table, the diameter of Pd was the key factor. Decreasing the diameter of the catalyst means more active sites can be exposed to the reaction system. Comparison with the TOF value of different catalyst revealed that the Pd-3 catalyst had a higher TOF value at a lower reaction temperature (120 °C), shorter reaction times (14 h), and lower Pd molar content (0.021 mol%) as compared to other supported Pd-based catalysts such as Pd loaded on mesoporous silica or TiO₂ [5]. The activity of Pd on carbon nanofiber [27] was higher than that of the Pd-3 catalyst, but carbon nanofiber was not as effective as Fe₃O₄@γ-Al₂O₃ in terms of the separation from the reaction systems, stability, and recyclability.

3.3. Relationship between the solvents, substrates and the catalytic performance of the catalyst

The condition of Heck reaction was rigorous, requiring an argon atmosphere to avoid the Pd leaching while maintaining the high activity in an anhydrous environment, and phosphine ligands to stabilize the catalyst, but the phosphine ligands are toxic and should be avoided. The solvents were often DMF

Table 2
Heck reaction activities of Pd-3 catalysts under different reaction conditions^a

Entry	Temperature (°C)	Base	Conversion (%)	Yield (%)	Selectivity (%)
1	90	Na ₂ CO ₃	19.7	17.2	87.3
2	100	Na ₂ CO ₃	47.7	43.9	92.0
3	110	Na ₂ CO ₃	75.2	70.5	93.8
4	120	Na ₂ CO ₃	96.8	91.2	94.2
5	120	Et ₃ N ^b	82.6	76.9	93.1
6	120	NaOAc	94.6	88.2	93.2

^a Reaction system: 20 mmol bromobenzene, 30 mmol styrene, 24 mmol base, 10 mmol dodecane, 40 mL NMP; reaction time: 14 h; catalyst: 0.01 g Pd-3 (4.5 wt%).

^b Et₃N: triethylamine.

Table 3

Comparison of the activity and reaction conditions of supported Pd catalysts in the Heck reaction of bromobenzene with styrene published in the literature.

Catalyst	Pd diameter (nm)	Catalyst (mol% Pd) ^a	Temperature (°C)	Time (h)	Yield (%)	TOF ^b	Reference
Pd/mesoporous silica	~10	0.1	170	48	82	17.1	[28]
Pd/TiO ₂	5	0.5	140	24	92	7.7	[5]
Pd/carbon nanofiber	2-3	0.01	120	10	95	950.0	[27]
Fe ₃ O ₄ -NH ₂ -Pd	8.9	5	130	24	96	0.8	[29]
Pd-3	3-4	0.021	120	14	91.2	310.2	This paper

^a Moles of Pd/moles of bromobenzene.^b mol_{product} mol⁻¹ Catalyst h⁻¹.**Table 4**Heck reaction activities of Pd-3 catalysts under different reaction conditions.^a

Entry	Solvent	Conversion (%)	Selectivity (%)	Yield (%)
1	NMP	96.8	94.2	91.2
2	DMF	98.7	92.1	90.9
3	DMSO	100.0	94.2	94.2
4	DMAc	100.0	94.4	94.4

^a Reaction system: 20 mmol bromobenzene, 30 mmol styrene, 24 mmol base, 10 mmol dodecane, 40 mL solvent; reaction time: 12 h; catalyst: 0.01 g Pd-3 (4.5 wt%).

(*N,N*-dimethylformamide), DMAc (dimethylacetamide), NMP (*N*-methyl-2-pyrrolidone), DMSO (dimethyl sulfoxide), etc. In the coupling reaction, the organic groups of the substrates varied from hydrophilic groups to hydrophobic groups or from electron-withdrawing groups to electron donating groups. So the nature of the solvents and substrates can influence the catalytic performance of the catalyst. Commonly, a catalyst had a high activity only in a specific solvent [5,30]. In contrast, our Pd-3 catalyst was suitable for most of the common solvents with a high conversion and yield, as shown in Table 4.

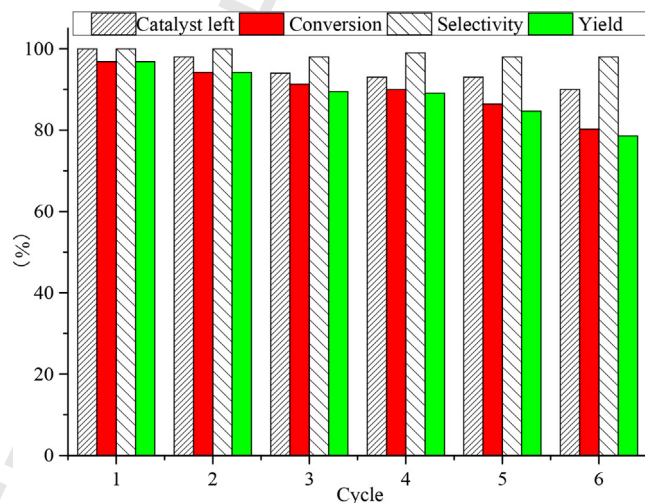
The effects of substituted groups in substrates were also examined. As illustrated in Table 5, the conversion of substrates with electron withdrawing groups in the *para*-position, at entry 1 to entry 2, was much higher than the substrates with electron donating groups, at entry 4 to entry 5. This result was the same as the other supported Pd catalysts result, which could be explained by the fact that the electron-withdrawing groups facilitate the oxidative addition during the Heck reaction [31]. When the olefin changed from styrene to straight-chain olefins, such as butyl acrylate or methyl acrylate, the conversion of bromobenzene decreased under the same reaction conditions, as shown at entry 6 to entry 7.

3.4. Stability and reusability of Pd/Fe₃O₄@γ-Al₂O₃

For practical application in the Heck reaction, the shelf life of the heterogeneous catalysts and their reusability are very

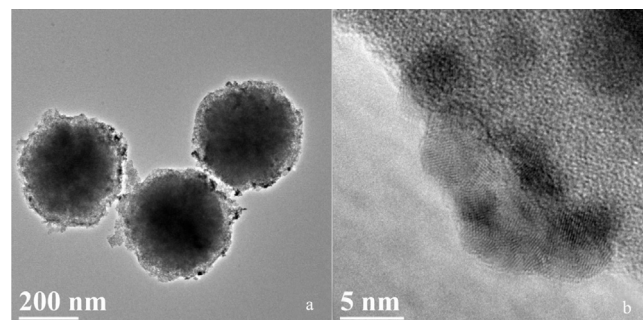
Table 5Heck reaction of various aryl bromides with different olefins catalyzed by Pd-3.^a

Entry	R	R ¹	Conversion (%)	Yield (%)
1	COCH ₃	C ₆ H ₆	100.0	95.8
2	NO ₂	C ₆ H ₆	100.0	96.1
3	H	C ₆ H ₆	88.8	82.4
4	OCH ₃	C ₆ H ₆	67.2	65.5
5	NH ₂	C ₆ H ₆	60.2	58.6
6	H	COO <i>i</i> -Bu	79.7	75.5
7	H	COOCH ₃	83.6	78.5

^a Reaction system: 20 mmol haloaromatic, 30 mmol olefin, 24 mmol base, 10 mmol dodecane, 40 mL NMP; reaction time: 12 h; catalyst: 0.01 g Pd-3 (4.5 wt%).**Fig. 6.** Recycling of the Pd-3 catalyst in Heck reaction.

important factors. Here our Pd-3 catalyst was reused for six times, each time after reaction the catalyst was separated from the reaction system by a permanent magnet, and the collected catalyst was washed with tetrahydrofuran and dried under vacuum at 60 °C for 12 h; catalyst loss was measured by precision electronic balance, then the catalyst was used in the next cycling under the same reaction conditions and giving 94.2%, 89.4%, 89.1%, 84.7% and 78.6% isolated yield for the second, third, fourth, fifth and sixth runs, respectively, as shown in Fig. 6.

Fig. 6 also shows that the weight loss of the catalyst was only 2% or less in each regeneration process, and the total weight loss of the catalyst was only 10% after six cycles. A baseline loss may be unavoidable in the regenerate process and the Pd leaching, which is the reason that the catalyst activity dropped each cycle. The conversion of bromobenzene decreased as the catalyst weight decreased, but remained above 80% with selectivity remaining at 100% after being used for six times. After use, the catalyst was dissolved in concentrated nitric acid and analyzed by inductively coupled plasma mass spectrometry (ICP-MS) to determine the

**Fig. 7.** TEM images of the Pd-3 catalyst recycled for six times in Heck reaction.

content of Pd (0.301 mmol/g). After being used six times, the core-shell structure and the γ -Al₂O₃ were retained. These were characterized by TEM as shown in Fig. 7. Parts of the Pd clusters were aggregated, maybe that was one of the reasons that the catalytic activity decreased compared to the fresh catalyst [27,32]. However, during the six runs of reusing process the Pd-3 catalyst retained the high activity and magnetic reusability.

4. Conclusion

In summary, we had synthesized magnetic Fe₃O₄@ γ -Al₂O₃ microspheres with core-shell structures by a coating and calcining process on inorganic magnetic core (Fe₃O₄) followed by loading Pd active component on the surface of the Fe₃O₄@ γ -Al₂O₃ microspheres by reducing PdCl₂. The catalyst of Pd was highly dispersed on the surface of the Fe₃O₄@ γ -Al₂O₃ microspheres with a diameter of 3–4 nm. Using the Pd/Fe₃O₄@ γ -Al₂O₃ (4.5 wt%) catalyst, the conversion of bromobenzene and the yield of product of about 96.8% and 91.2%, respectively, were obtained at 120 °C in 14 h. After being recycled for six times, the catalyst gave a conversion of bromobenzene of above 80% and the recovery of the catalyst was above 90%. The nano-Pd particles were kept well dispersed in the used Pd/Fe₃O₄@ γ -Al₂O₃ catalyst, which show a good applicability in industry.

Q2 Uncited reference

[33].

Acknowledgment

Financial support from the National Natural Science Foundation of China (No. 21173018) is gratefully acknowledged.

References

[1] T. Mizoroki, K. Mori, A. Ozaki, Arylation of olefin with aryl iodide catalyzed by palladium, *Bull. Chem. Soc. Jpn.* 44 (1971) 581.
[2] R.F. Heck, J.P. Nolley, Palladium-catalyzed vinylic hydrogen substitution reactions with aryl, benzyl, and styryl halides, *J. Org. Chem.* 37 (1972) 2320–2322.
[3] R.A. Sheldon, H. van Bekkum, *Fine Chemicals Through Heterogeneous Catalysis*, Wiley-VCH, Weinheim, 2001.
[4] L.X. Yin, J. Liebscher, Carbon-carbon coupling reactions catalyzed by heterogeneous palladium catalysts, *Chem. Rev.* 107 (2007) 133–173.
[5] Z.H. Li, J. Chen, W.P. Su, M.C. Hong, A titania-supported highly dispersed palladium nano-catalyst generated via in situ reduction for efficient Heck coupling reaction, *J. Mol. Catal. A: Chem.* 328 (2010) 93–98.
[6] P.Y. Wang, X.P. Zheng, Pd/SBA-15 nanocomposite: synthesis, structure and catalytic properties in Heck reactions, *Powder Technol.* 210 (2011) 115–121.
[7] X.J. Feng, M. Yan, X. Zhang, M. Bao, Preparation and application of SBA-15-supported palladium catalyst for Heck reaction in supercritical carbon dioxide, *Chin. Chem. Lett.* 22 (2011) 643–646.
[8] M. Bakherad, S. Jajarmi, A dithione-functionalized polystyrene resin-supported Pd(II) complex as an effective catalyst for Suzuki, Heck, and copper-free Sonogashira reactions under aerobic conditions in water, *J. Mol. Catal. A: Chem.* 370 (2013) 152–159.
[9] A. Molnar, A. Papp, Efficient heterogeneous palladium-montmorillonite catalysts for heck coupling of aryl bromides and chlorides, *Syn. Lett.* 18 (2006) 3130–3134.
[10] J.H. Ji, S.F. Ji, W. Yang, C.Y. Li, Preparation and application of magnetic Fe₃O₄ nanocrystalline, *Prog. Chem.* 22 (2010) 1566–1574.

[11] B. Baruwati, D. Guin, S.V. Manorama, Pd on surface-modified NiFe₂O₄ nanoparticles: a magnetically recoverable catalyst for Suzuki and Heck reactions, *Org. Lett.* 9 (26) (2007) 5377–5380.
[12] J. Park, J. Joo, S.G. Kwon, Y. Jang, T. Hyeon, Synthesis of monodisperse spherical nanocrystals, *Angew. Chem. Int. Ed.* 46 (2007) 4630–4660.
[13] H.F. Liu, S.F. Ji, H. Yang, H. Zhang, M. Tang, Ultrasonic-assisted ultra-rapid synthesis of monodisperse meso-SiO₂@Fe₃O₄ microspheres with enhanced mesoporous structure, *Ultrason. Sonochem.* 21 (2014) 505–512.
[14] H. Zhang, D.L. Liu, L.L. Zeng, M. Li, β -Cyclodextrin assisted one-pot synthesis of mesoporous magnetic Fe₃O₄@C and their excellent performance for the removal of Cr (VI) from aqueous solutions, *Chin. Chem. Lett.* 24 (2013) 341–343.
[15] Y. Li, T.H. Leng, H.Q. Lin, et al., Preparation of Fe₃O₄@ZrO₂ core-shell microspheres as affinity probes for selective enrichment and direct determination of phosphopeptides using matrix-assisted laser desorption ionization mass spectrometry, *J. Proteome Res.* 6 (2007) 4498–4510.
[16] J. Jin, F. Yang, F.W. Zhang, et al., 2,2-(Phenylazanediy) diacetic acid modified Fe₃O₄@PEI for selective removal of cadmium ions from blood, *Nanoscale* 4 (2012) 733–737.
[17] X.X. Yang, E. Larry, L.E. Erickson, K.L. Hohn, Sol-gel Cu-Al₂O₃ adsorbents for selective adsorption of thiophene out of hydrocarbon, *Ind. Eng. Chem. Res.* 45 (2006) 6169–6174.
[18] S.A. Sadaphal, A.H. Kategaonkar, V.B. Labade, M.S. Shingare, Synthesis of bis (indolyl) methanes using aluminium oxide (acidic) in dry media, *Chin. Chem. Lett.* 21 (2010) 39–42.
[19] H. Tajizadegan, M. Rashidzadeh, M. Jafari, R.E. Kahrizsangi, Novel ZnO-Al₂O₃ composite particles as sorbent for low temperature H₂S removal, *Chin. Chem. Lett.* 24 (2013) 167–169.
[20] J. Huang, Y. Wang, J.M. Zheng, W.L. Dai, K.N. Fan, Influence of support surface basicity and gold particle size on catalytic activity of Au/ γ -AlOOH and Au/ γ -Al₂O₃ catalyst in aerobic oxidation α , ω -diols to lactones, *Appl. Catal. B: Environ.* 103 (2011) 343–350.
[21] M.I. Cobo, J.A. Conesa, C.M. Correa, The effect of NaOH on the liquid-phase hydrodechlorination of dioxins over Pd/ γ -Al₂O₃, *J. Phys. Chem. A* 112 (2008) 8715–8722.
[22] B.B. Chen, X.B. Zhu, M. Croker, Y. Wang, C. Shi, Complete oxidation of formaldehyde at ambient temperature over γ -Al₂O₃ supported Au catalyst, *Catal. Commun.* 42 (2013) 93–97.
[23] X. Li, C.H. Xu, C.Q. Liu, Y. Chen, J.Y. Liu, Synthesis of pyrazinyl compounds from glycerol and 1,2-propanediamine over Cu-TiO₂ catalysts supported on γ -Al₂O₃, *Chin. Chem. Lett.* 24 (2013) 751–754.
[24] H.F. Liu, S.F. Ji, Y.Y. Zheng, M. Li, H. Yang, Modified solvothermal synthesis of magnetic microspheres with multifunctional surfactant cetyltrimethyl ammonium bromide and directly coated mesoporous shell, *Powder Technol.* 246 (2013) 520–529.
[25] Y.Y. Zheng, S.F. Ji, H.F. Liu, M. Li, H. Yang, Synthesis of mesoporous γ -AlOOH@Fe₃O₄ magnetic nanomicrospheres, *Particuology* 10 (2012) 751–758.
[26] W. Li, B.L. Zhang, X.J. Li, H.P. Zhang, Q.Y. Zhang, Preparation and characterization of novel immobilized Fe₃O₄@SiO₂@mSiO₂-Pd(0) catalyst with large pore-size mesoporous for Suzuki coupling reaction, *Appl. Catal. A: Gen.* 459 (2013) 65–72.
[27] G.B. Donna, Reaction progress kinetic analysis: a powerful methodology for mechanistic studies of complex catalytic reactions, *Angew. Chem. Int. Ed.* 44 (2005) 4302–4320.
[28] J. Zhu, J.H. Zhou, T.J. Zhao, et al., Carbon nanofiber-supported palladium nanoparticles as potential recyclable catalysts for the Heck reaction, *Appl. Catal. A: Gen.* 353 (2009) 243–250.
[29] C.P. Mehnert, D.W. Weaver, J.Y. Yin, Heterogeneous Heck catalysis with palladium-grafted molecular sieves, *J. Am. Chem. Soc.* 120 (1998) 12289–12296.
[30] F.W. Zhang, J. Jin, X. Zhong, et al., Pd immobilized on amine functionalized magnetite nanoparticles: a novel and highly active catalyst for hydrogenation and Heck reactions, *Green Chem.* 13 (2011) 1238–1243.
[31] J.A. Bennett, I.P. Mikheenko, K. Deplanche, et al., Nanoparticles of palladium supported on bacterial biomass: new re-usable heterogeneous catalyst with comparable activity to homogeneous colloidal Pd in the Heck reaction, *Appl. Catal. A: Environ.* 140 (2013) 700–707.
[32] A. Balanta, C. Godard, C. Claver, Cross coupling reactions in organic synthesis themed issue, *Chem. Soc. Rev.* 40 (2011) 4973–4985.
[33] M.Y. Zhu, G.W. Diao, Magnetically recyclable Pd nanoparticles immobilized on magnetic Fe₃O₄@C nanocomposites: preparation, characterization, and their catalytic activity toward Suzuki and Heck coupling reactions, *J. Phys. Chem.* 115 (2011) 24743–24749.

341
342
343
344
345
346
347
348
349
350
351
352
353
354
355
356
357
358
359
360
361
362
363
364
365
366
367
368
369
370
371
372
373
374
375
376
377
378
379
380
381
382
383
384
385
386
387
388
389
390
391
392
393
394
395
396
397
398
399
400
401
402
403
404
405
406
407
408
409
410